The Astrophysical Journal Letters, 895:L38 (5pp), 2020 June 1 https://doi.org/10.3847/2041-8213/ab922c

A Redshift for the First Einstein Ring, MG 1131+0456

Daniel Stern[1] and Dominic J. Walton[2]
[1] Jet Propulsion Laboratory, California Institute of Technology, 4800 Oak Grove Drive, Pasadena, CA 91109, USA; daniel.k.stern@jpl.nasa.gov
[2] Institute of Astronomy, University of Cambridge, Madingley Road, Cambridge CB3 0HA, UK
Received 2020 April 5; revised 2020 May 4; accepted 2020 May 5; published 2020 June 1

Abstract

MG 1131+0456 is a radio-selected gravitational lens, and is the first known Einstein ring. Discovered in 1988, the system consists of a bright ($S_{74\,\mathrm{MHz}} = 3.7$ Jy) radio source imaged into a ring and two compact, flat-spectrum components separated by 2.″1. The ring is optically faint ($R = 23.3$), rising steeply into the near- and mid-infrared ($K = 17.8$; W2 = 13.4). The system has been intensively studied in the intervening years, including high-resolution radio imaging, radio monitoring, and near-infrared imaging with Hubble and Keck. The lensing galaxy is at $z_l = 0.844$. However, to date, no spectroscopic redshift had been reported for the lensed source. Using archival Keck data from 1997, we report the robust detection of a single narrow emission line at 5438 Å, which we associate with C III] λ1909 Å from a type-2 quasar at $z_s = 1.849$. Support for this redshift identification comes from weaker emission associated with C IV λ1549 Å and He II λ1640 Å, typical of type-2 quasars, as well as the lack of emission lines in archival near-infrared Keck spectroscopy. We also present, for the first time, Cycle 1 Chandra observations of MG 1131+0456, which clearly resolves into two point sources with a combined flux of $\sim 10^{-13}$ erg cm^{-2} s^{-1} and a best-fit column density of $\sim 3 \times 10^{22}$ cm^{-2}. We suggest a new method to identify candidate lensed active galactic nuclei from low-resolution X-ray surveys such as eROSITA by targeting sources that have anomalously high X-ray luminosity given their mid-infrared luminosity.

Unified Astronomy Thesaurus concepts: Gravitational lensing (670)

1. Introduction

MG 1131+0456 was the first discovered Einstein ring (Hewitt et al. 1988), identified shortly after the first discovery of lensed arcs in rich galaxy clusters (Lynds & Petrosian 1987; Soucail et al. 1987) and about a decade after the first discovery of a lensed quasar (Walsh et al. 1979). The unusual radio structure consists of an elliptical ring with major and minor axes of 2.″2 and 1.″6, respectively, accompanied by a pair of compact sources slightly offset from the ring (~0.″3 to the southwest). A low surface brightness component is also evident to the southwest of the ring. Shortly after its discovery, MG 1131+0456 was successfully modeled by Kochanek et al. (1989) to be a gravitationally lensed radio galaxy, where the radio jet aligns with the astroid caustic of the foreground lens and produces an Einstein ring (Einstein 1936), the radio core is slightly misaligned with the lensing galaxy, producing the pair of compact sources, and the low surface brightness component to the southwest is a radio lobe. Chen & Hewitt (1993) and Hewitt et al. (1995) present improved, multifrequency radio images of MG 1131+0456, showing the compact sources to be flat-spectrum sources, as expected for radio cores, and that these compact sources are weakly variable. The radio flux rises to lower frequencies, with $S_{74\,\mathrm{MHz}} = 3.7 \pm 0.4$ Jy (Cohen et al. 2007).

The system (i.e., lens plus source) is faint at optical wavelengths, $V = 23.0$, and rises steeply in the near-infrared, $K = 16.0$ (Annis 1992). Separating the lens from the source reveals the background Einstein ring to be extremely red, with $R = 23.3$ and $K = 17.8$ (Annis 1992). Indeed, Larkin et al. (1994) noted MG 1131+0456 was among the first of a new class of extremely red objects ($R - K \gtrsim 6$; e.g., Elston et al. 1988), and suggested the red colors might be due to dust extinction in the lensing galaxy. However, they also highlighted various objections to that hypothesis; e.g., the lensing galaxy appeared to be early-type, and such galaxies typically do not contain much dust, particularly on the $\geqslant$10 kpc scale separating the lensing paths of the background source. Based on near-infrared imaging from the Hubble Space Telescope and revised multi-wavelength lens modeling of this system, Kochanek et al. (2000a) demonstrated that the host galaxy of MG 1131+0456 is an intrinsically red galaxy, as suggested by Annis & Luppino (1993), and that tidal perturbations from nearby galaxies can explain the elongated shape of the Einstein ring, as suggested by Chen et al. (1995).

Based on optical to near-infrared imaging and modeling of the gravitational lens, several authors concluded that the lens was an early-type galaxy at $z_l = 0.7$–0.9 (e.g., Larkin et al. 1994; Kochanek et al. 2000b), consistent with the tentative $z_l = 0.85$ found by Hammer et al. (1991). Tonry & Kochanek (2000) presented an optical spectrum of the system obtained with the Keck 2 telescope, conclusively demonstrating that the lensing galaxy is an early-type galaxy at $z_l = 0.844$ with [O II] $\lambda\lambda$3727 Å emission, CaHK absorption, and a strong D4000 break. From the lens model, they argue that the source redshift for MG 1131+0456 is at $z_s > 1.9$. However, prior to this Letter, no spectroscopic redshift for the Einstein ring had been reported.

Here we report on a re-analysis of archival Keck observations of MG 1131+0456, which provide a spectroscopic redshift for the lensed radio galaxy. We also present archival observations with Chandra (Weisskopf et al. 2002) that resolve the source into two bright X-ray point sources, associated with the lensed radio core. Throughout this Letter, magnitudes are reported in the Vega system. When computing luminosities, we adopt the ΛCDM concordance cosmology: $H_0 = 70$ km s^{-1} Mpc^{-1}, $\Omega_M = 0.3$, and $\Omega_\Lambda = 0.7$.

Table 1
Archival Keck Spectroscopy of MG 1131+0456

UT Date	Inst.	Position Angle (PA) (deg)	Exposure (s)	$\lambda\lambda$ (μm)	PI
1997 Mar 31	LRIS	45	3300	0.37–0.87	Tonry
1999 May 11	LRIS	63	5400	0.68–0.84	Tonry
2000 Apr 12	NIRSPEC	116	1800	1.14–1.38	Larkin
2000 Apr 12	NIRSPEC	117	600	2.00–2.38	Larkin
2002 Feb 8	ESI	93	5400	0.39–1.02	Koopmans
2007 Jan 27	NIRSPEC	60	2400	1.43–1.81	Canalizo
2007 Jan 27	NIRSPEC	60	2400	1.95–2.30	Canalizo

Note. $\lambda\lambda$ lists the wavelength range covered by the observations.

2. Observations and Analysis

We re-discovered MG 1131+0456 while searching for lensed obscured quasars. While over 200 lensed quasars are currently known,[3] the number of known lensed obscured, or type-2, quasars is significantly smaller, potentially in the single digits despite the fact that most accreting black holes in the universe are obscured. Examples include MG 2016+112 at $z_s = 3.273$ (Lawrence et al. 1984), MG J0414+0534 at $z_s = 2.639$ (Hewitt et al. 1992), and PMN J0134−0931 at $z_s = 2.216$ (Winn et al. 2002). Notably, all of these were radio selected. Mimicking the long delay between the discovery of distant, radio-loud, type-2 quasars (i.e., high-redshift radio galaxies; e.g., Spinrad 1982) and the discovery of distant, radio-quiet, type-2 quasars (e.g., Stern et al. 2002), only more recently have lensed, radio-quiet, type-2 quasars been identified, with examples including MACS J212919.9−074218 at $z_s = 1.212$ (Stern et al. 2010) and W2M J1042+1641 at $z_s = 2.517$ (Glikman et al. 2020). Both those discoveries were serendipitous.

In order to find additional lensed obscured quasars, we correlated known galaxy–galaxy lenses from the Master Lens Database (L. Moustakas et al. 2020, in preparation) with mid-infrared photometry from the Wide-field Infrared Survey Explorer (WISE; Wright et al. 2010). We then identified which systems included an active galaxy based on red colors between the first two WISE bands, W1 (3.4 μm) and W2 (4.6 μm); namely, W1–W2 $\geqslant 0.8$ is a highly effective and efficient criterion for identifying both obscured and unobscured quasars (e.g., Stern et al. 2012; Assef et al. 2013). Given the $\sim 6''$ resolution of WISE, this selection could identify either lensed quasars or systems where a quasar is responsible for the lensing; both scenarios are scientifically valuable (e.g., Courbin et al. 2012). Only one high-quality galaxy–galaxy lens (i.e., "lensgrade" = A) had such red WISE colors: MG 1131+0456.

The re-discovery of this interesting, bright, mid-infrared source (W2 = 13.40) with extremely red WISE colors (W1–W2 = 0.93) inspired a search of the archives to learn more about this source that had attracted significant attention after its discovery three decades ago, but had largely been forgotten for the past two decades.

2.1. Keck

MG 1131+0456 was observed by the Keck telescopes in the late 1990 s. Examples of similar Keck observations of high-redshift radio galaxies in that era appear in Stern (1999). Table 1 presents a list of all publicly available Keck spectroscopy of MG 1131+0456 in the Keck archive. Other than the 1999 observations that appear in Tonry & Kochanek (2000), these data have not previously appeared in the literature.

We have analyzed all these data. Continuum is detected in all cases, coming from the lens for the optical data and primarily from the background radio galaxy source for the near-infrared data. As noted earlier, the Low Resolution Imaging Spectrograph (LRIS; Oke et al. 1995) clearly reveals the lens to be an early-type galaxy with [O II] emission (Tonry & Kochanek 2000).

The only observation in which a spectral feature is detected from the source is the first observation, obtained with LRIS in 1997. Those data, presented in Figure 1, were obtained through the $1\farcs0$ slit at a position angle (PA) = 45° with the 300 $\ell\,\mathrm{mm}^{-1}$ grating ($\lambda_{\mathrm{blaze}} = 5000$ Å; resolving power $R \equiv \lambda/\Delta\lambda \approx 600$ for objects filling the slit). This PA is slightly offset from the 63° angle of the radio cores. At the time, LRIS was a single-beam spectrograph; a blue arm has since been added. Two observations were obtained, with exposure times of 1500 s and 1800 s. We processed the spectra using standard techniques, and flux calibrated the combined, extracted spectrum using an archival sensitivity function obtained through the same grating.

An emission line at 5438 Å is well detected in both individual exposures, offset by $1''$ from the lensing galaxy as expected given the geometry of the Einstein ring and radio cores described in Section 1. No continuum is detected from the lensed radio galaxy, and a weaker emission line is detected at 4667 Å. As shown in Figure 1, we associate these lines with C III] λ1909 Å and He II λ1640 Å at $z_s = 1.849 \pm 0.002$ (the uncertainty is a conservative estimate, reflecting statistical uncertainties, systematic wavelength calibration uncertainties, and kinematics in the source). Another weak feature is also evident in the extracted spectrum corresponding to C IV λ1549 Å. These high-ionization, narrow, high equivalent width emission lines are typical of luminous, obscured active galactic nuclei (AGNs), such as high-redshift radio galaxies (e.g., Stern et al. 1999) and type-2 quasars (e.g., Stern et al. 2002). As detailed below, the redshift we derive for MG 1131+0456 places other key emission features at wavelengths challenging or inaccessible from the ground.

At observed optical wavelengths, we might have expected to see Lyα and the Mg II $\lambda\lambda$2800 Å doublet. Lyα, typically one of the brightest features in an active galaxy, is expected at 3464 Å. Though accessible from the ground, none of the Keck

[3] As of 2020 March 14, the Gravitationally Lensed Quasar Database, https://web1.ast.cam.ac.uk/ioa/research/lensedquasars, contains 219 known lensed quasars.

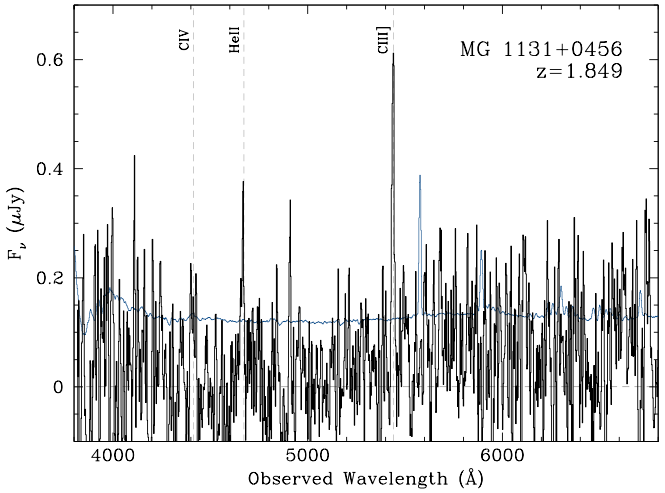

Figure 1. Keck/LRIS observation of MG 1131+0456 from 1997 March in black; the blue line shows the 1σ error spectrum. Spectra were extracted with a $1\farcs0$ width aperture and smoothed with a 3 pixel boxcar. A strong emission line is present at 5438 Å, associated with C III] λ1909 Å, with supporting weaker lines associated with C IV λ1549 Å and He II λ1640 Å also detected. The spectrum is typical of type-2 quasars.

observations to date reach such a blue wavelength (see Table 1). Mg II is expected at 7977 Å, which is a wavelength that was sampled by multiple archival observations, albeit in a noisier part of the spectrum due to telluric OH emission. In the composite MG radio galaxy spectrum of Stern et al. (1999), C III] and Mg II have comparable strength, though the composite radio galaxy spectrum presented in McCarthy (1993) has C III] roughly twice as strong as Mg II, and the Seyfert II composite from Ferland & Osterbrock (1986) has C III] three times as strong as Mg II. We ascribe the non-detection of Mg II from the lensed galaxy to a combination of a more Seyfert II-like line ratio and elevated noise due to telluric emission at redder optical wavelengths. Finally, we note that the 2002 observations with the Echellette Spectrograph and Imager (ESI; Sheinis et al. 2002) do not detect the C III] line, likely due to a combination of a sub-optimal position angle for those observations and the line being at a wavelength where the light is split across two orders of this cross-dispersed spectrograph.

At observed near-infrared wavelengths, we might have expected to see [O II], Hβ λ4861 Å, [O III] $\lambda\lambda$4959, 5007 Å, and/or Hα λ6563 Å. [O II] is expected at 1.06 μm, which is blueward of the NIRSPEC observations. The Hβ/[O III] complex is redshifted to 1.38–1.42 μm, which is between the *J*- and *H*-bands, and in a wavelength range strongly affected by atmospheric absorption. Hα, usually one of the strongest lines in a galaxy or active galaxy, is redshifted to 1.87 μm, which is between the *H*- and *K*-bands, and is also in a wavelength range strongly affected by atmospheric absorption. The non-detection of spectral features in archival near-infrared Keck spectra that clearly detect strong continuum lends further support to our redshift assignment and likely explains why a redshift had not previously been reported for MG 1131+0456 despite multiple observations over decades.

2.2. *Chandra*

Chandra observed MG 1131+0456 with its ACIS-S detector (Garmire et al. 2003) on two occasions beginning less than a year after launch (OBSIDs 423 and 424, taken on 2000 May 2 and 2000 December 15, respectively), each with an exposure of ~7 ks. We reprocessed both observations with CIAO v4.11 and the latest Chandra calibration files. Cleaned event files were generated with the CHANDRA_REPRO script, with the EDSER sub-pixel event re-positioning algorithm enabled (Li et al. 2004). Following previous work (e.g., Reynolds et al. 2014), the cleaned event files were re-binned to 1/8 of the ACIS pixel size before smoothing with a Gaussian ($0\farcs25$ FWHM) for visualization and to define our source regions. MG 1131+0456 is clearly resolved into two X-ray sources separated by $2''$ by Chandra (Figure 2), similar to the two radio cores reported by Hewitt et al. (1988), one to the northeast (image A) and one to the southwest (image B). For each epoch, we initially extracted individual spectra from each of the two images with the SPECEXTRACT script, which also generated the relevant instrumental response files. Source events were extracted from circular regions of radius $1\farcs25$ (ensuring the two extraction regions do not overlap), while background was estimated from much larger regions of blank sky on the same chip as MG 1131+0456 (radius $27''$).

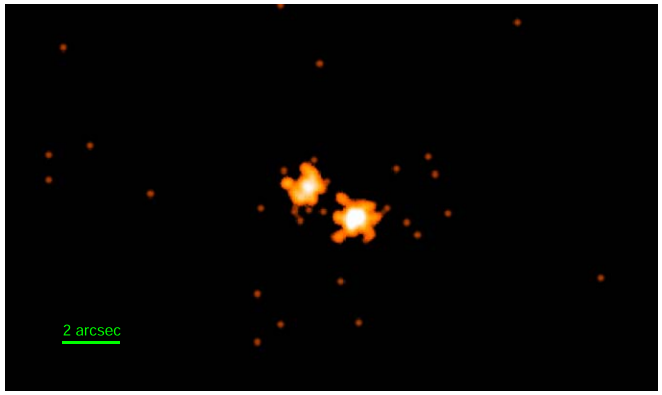

Figure 2. Chandra X-ray image of MG 1131+0456, combining OBSIDs 423 and 424. North is up and east is to the left. MG 1131+0456 is clearly resolved into two point sources, image A to the northeast and image B to the southwest.

We modeled these four spectra with a simple absorbed power-law continuum, allowing for absorption both from our own Galaxy (with the column fixed to $N_{\rm H,Gal} = 2.87 \times 10^{20}$ cm^{-2}; Kalberla et al. 2005) and intrinsic to the source (i.e., at $z_s = 1.849$), adopting the solar abundance set reported in Wilms et al. (2000). Each spectrum was grouped to a minimum of 1 count per bin, and the data were analyzed by reducing the Cash statistic (Cash 1979); the Chandra data are modeled over the 0.35–8.0 keV bandpass in the observed frame, corresponding to rest-frame energies of ~1–23 keV. The spectral parameters are consistent for all four of the individual spectra, although we note that the signal-to-noise of each is fairly poor, as they are comprised of only 26–56 counts (165 ± 13 counts in total, combining both images and both epochs). We also find that, within the limitations of the available data and assuming common spectral parameters, both the image flux ratios and the combined image fluxes are consistent between the two epochs. In the X-ray band, image B is 1.5 ± 0.4 times brighter than image A, consistent with the radio core flux ratios of 1.23 ± 0.10 at 15 GHz and 1.38 ± 0.22 at 22 GHz found by Chen & Hewitt (1993).

Given this, we combined the data from both images and both epochs to produce an average spectrum for MG 1131+0456 (using ADDASCASPEC). Fitting this data with the above absorbed power-law model, we find an intrinsic absorption

column of $N_{\rm H} = 3.0^{+1.7}_{-1.5} \times 10^{22}$ cm^{-2} and a photon index of $\Gamma = 1.7^{+0.4}_{-0.3}$. The latter is a typical X-ray continuum slope for AGNs. For example, based on a study of the broadband X-ray properties of 838 AGNs from the 70-month Swift/BAT all-sky survey, Ricci et al. (2017) find median values of $\Gamma = 1.78 \pm 0.01$ for non-blazar AGNs and $\Gamma = 1.54 \pm 0.05$ for flat-spectrum radio quasars. We also compute the combined 2–10 keV flux (rest-frame) of the two images, mimicking what would be seen by observatories that do not have the spatial resolution of Chandra. After correcting for the line-of-sight absorption, we find $F_{\rm A+B;2-10} = (5.5 \pm 1.0) \times 10^{-14}$ erg cm^{-2} s^{-1}. Similarly, the total observed flux (prior to any absorption correction) of the combined images over the full Chandra band (0.35–8 keV observed frame, 1–23 keV rest-frame) is $F_{\rm A+B;1-23} = (8.7 \pm 1.8) \times 10^{-14}$ erg cm^{-2} s^{-1}.

3. Discussion

With the redshift of MG 1131+0456 now known, we can do some rough calculations of the properties of the lensing galaxy. Approximating the Einstein ring as a circle of diameter 1.″9, the radius of an Einstein ring, $\theta_{\rm E}$ (in radians) is related to the projected mass enclosed by the Einstein radius, $M_{\rm E}$ by

$$\theta_{\rm E} = \sqrt{\frac{4\,G\,M_{\rm E}}{c^2}\,\frac{D_{\rm LS}}{D_{\rm S}\,D_{\rm L}}},$$

where $D_{\rm S}$ ($D_{\rm L}$) is the angular diameter distance to the source (lens), and $D_{\rm LS}$ is the angular diameter distance between the source and lens. For a flat universe (i.e., $\Omega_{\rm M} + \Omega_\Lambda = 1$), $D_{\rm LS} = D_{\rm S} - D_{\rm L}\,(1 + z_l)/(1 + z_s)$. For the MG 1131+0456 lens, we find $M_{\rm E} = 4.2 \times 10^{11}\,M_\odot$. From Hubble near-infrared imaging, Kochanek et al. (2000b) found that the lensing galaxy is well-fit by a de Vaucouleurs profile with an effective radius $R_e = 0.''7$, which is much less than the Einstein radius. Observed I-band roughly corresponds to rest-frame B-band for the lensing galaxy, so the observed I-band magnitude of the lensing galaxy, $I = 21.04$ (Kochanek et al. 2000b), corresponds to a rest-frame B-band luminosity of $L_{\rm B} = 1.7 \times 10^{11}\,L_{\rm B,\odot}$. The implied mass-to-light ratio of the lensing galaxy enclosed by the Einstein ring is then $M_{\rm E}/L_{\rm B} \approx 2.5\,M_\odot/L_{\rm B,\odot}$, which is low for local early-type galaxies (e.g., Gerhard et al. 2001), but consistent with early-type galaxies at higher redshift (e.g., van der Wel et al. 2005).

Figure 3 shows rest-frame 2–10 keV X-ray luminosity against rest-frame 6 μm luminosity for AGNs over a wide range in luminosity. At low luminosities, the relation is roughly linear, while at high luminosities, the 2–10 keV X-ray emission essentially saturates as the corona more effectively cools and softens when the accretion disk thermal emission increases (e.g., Brightman et al. 2013). Also shown on this figure are the observed and intrinsic luminosities of MG 1131+0456. The mid-infrared luminosity is derived by extrapolating the observed WISE photometry. WISE does not resolve the system, so this combines the flux from the lens and the source, though at these wavelengths, the early-type lensing galaxy is strongly overpowered by the AGN. The X-ray luminosity is the sum of both point sources, to provide a consistent comparison with the WISE data. With the source redshift now determined, MG 1131+0456 warrants a full lensing model, including sheer from galaxies close to the line of sight as well as an ellipsoidal

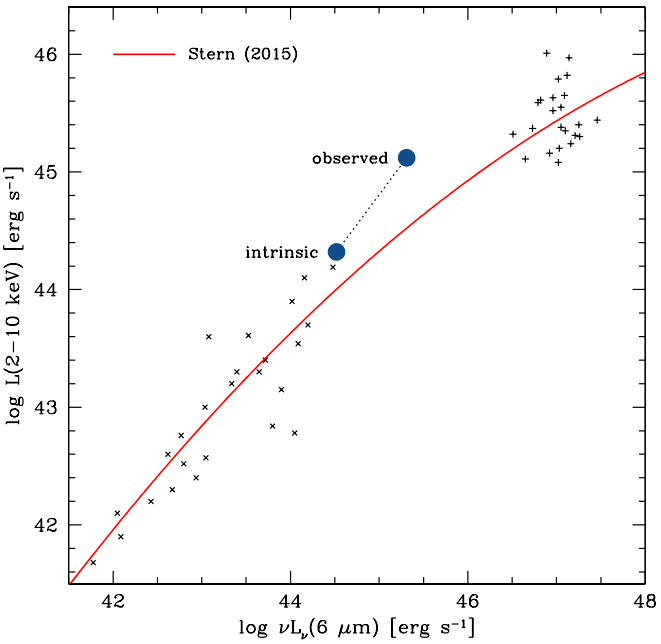

Figure 3. Rest-frame 2–10 keV X-ray luminosity against rest-frame 6 μm luminosity for AGNs over a wide range in luminosity, with the relation from Stern (2015) indicated as red solid curve. Black crosses show local Seyfert galaxies from Horst et al. (2008) and Gandhi et al. (2009), while black plus signs show luminous quasars from Just et al. (2007). Large circles show observed and lensing-corrected values for MG 1131+0456. Intrinsically, the radio galaxy lies close to observed relation, at a luminosity where the relation is roughly linear. However, the observed value lies far above the relation, suggesting a new method to identify lensed AGNs.

model of the lensing galaxy. In lieu of a full model, which is beyond the scope of this Letter, we instead adopt an approximate 2 mag magnification based on the optical and near-infrared magnifications in Kochanek et al. (2000a). With this correction, MG 1131+0456 intrinsically resides close to the linear region of the X-ray-mid-infrared relation. Figure 3 suggests a new way to identify candidate lensed AGNs from low-resolution, wide-area X-ray surveys such as eROSITA, by targeting sources which have an anomalously high X-ray luminosity given their mid-infrared luminosity.

With the redshift of MG 1131+0456, the first Einstein ring, now known, this opens up a range of follow-up observations and studies. Given the moderate absorption found from the X-ray analysis, the expectation is that MG 1131+0456 will have broad Balmer emission lines, similar to reddened quasars (e.g., Glikman et al. 2007). However, given the redshift of the source, this will require space-based observations. Longer wavelength emission line studies are also made feasible with the source redshift known, such as targeted ALMA or APEX studies of the CO sled, as well as [C I] and [C II] emission. Foremost, with the source redshift known, an updated lens model is called for. This would allow a range of studies, including improved measurements of the dark matter properties of the lensed galaxy.

We thank our colleagues, including Carlos De Breuck, Anna Nierenberg, and Nick Seymour, for their input and discussions of this source. In particular, we thank Leonidas Moustakas for providing access to the Master Lens Database. The work of D. S. was carried out at the Jet Propulsion Laboratory, California Institute of Technology, under a contract with NASA. D.J.W. acknowledges support from an STFC Ernest Rutherford

Fellowship. Based on observations at the W. M. Keck Observatory, which is operated as a scientific partnership among the University of California, the California Institute of Technology, and the National Aeronautics and Space Administration. The Observatory was made possible by the generous financial support of the W. M. Keck Foundation. The scientific results reported in this article are based in part on previously unpublished data obtained from the Chandra Data Archive.

Facilities: Chandra, Keck (LRIS).

ORCID iDs

Daniel Stern https://orcid.org/0000-0003-2686-9241
Dominic J. Walton https://orcid.org/0000-0001-5819-3552

References

Annis, J. 1992, ApJ, 391, 17
Annis, J., & Luppino, G. A. 1993, ApJL, 407, L69
Assef, R. J., Stern, D., Kochanek, C. S., et al. 2013, ApJ, 772, 26
Brightman, M., Silverman, J. D., Mainieri, V., et al. 2013, MNRAS, 433, 2485
Cash, W. 1979, ApJ, 228, 939
Chen, G. H., & Hewitt, J. N. 1993, AJ, 106, 5
Chen, G. H., Kochanek, C. S., & Hewitt, J. N. 1995, ApJ, 447, 62
Cohen, A. S., Lane, W. M., Cotton, W. D., et al. 2007, AJ, 134, 1245
Courbin, F., Faure, C., Djorgovski, S. G., et al. 2012, A&A, 540, 36
Einstein, A. 1936, Sci, 84, 506
Elston, R., Rieke, G. H., & Rieke, M. J. 1988, ApJL, 331, L77
Ferland, G. J., & Osterbrock, D. E. 1986, ApJ, 300, 658
Gandhi, P., Horst, H., Smette, A., et al. 2009, A&A, 502, 457
Garmire, G. P., Bautz, M. W., Ford, P. G., Nousek, J. A., & Ricker, G. R., Jr. 2003, Proc. SPIE, 4851, 28
Gerhard, O., Kronawitter, A., Saglia, R. P., & Bender, R. 2001, AJ, 121, 1936
Glikman, E., Helfand, D. J., White, R. L., et al. 2007, ApJ, 667, 673
Glikman, E., Rusu, C. E., Djorgovski, S. G., et al. 2020, ApJ, submitted, arXiv:1807.05434
Hammer, F., Le Févre, O., Angonin, M. C., et al. 1991, A&A, 250, L5
Hewitt, J. N., Chen, G. H., & Messier, M. D. 1995, AJ, 109, 1956
Hewitt, J. N., Turner, E. L., Lawrence, C. R., Schneider, D. P., & Brody, J. P. 1992, AJ, 104, 968
Hewitt, J. N., Turner, E. L., Schneider, D. P., et al. 1988, Natur, 333, 537
Horst, H., Gandhi, P., Smette, A., & Duschl, W. J. 2008, A&A, 479, 389
Just, D., Brandt, W. N., Shemmer, O., et al. 2007, ApJ, 665, 1004
Kalberla, P. M. W., Burton, W. B., Hartmann, D., et al. 2005, A&A, 440, 775
Kochanek, C. S., Blandford, R. D., Lawrence, C. R., & Narayan, R. 1989, MNRAS, 238, 43
Kochanek, C. S., Falco, E. E., Impey, C. D., et al. 2000a, ApJ, 535, 692
Kochanek, C. S., Falco, E. E., Impey, C. D., et al. 2000b, ApJ, 543, 131
Larkin, J. E., Matthews, K., Lawrence, C. R., et al. 1994, ApJL, 420, L9
Lawrence, C. R., Schneider, D. P., Schmidt, M., et al. 1984, Sci, 223, 46
Li, J., Kastner, J. H., Prigozhin, G. Y., et al. 2004, ApJ, 610, 1204
Lynds, R., & Petrosian, V. 1987, BAAS, 18, 1014
McCarthy, P. J. 1993, ARA&A, 31, 639
Oke, J. B., Cohen, J. G., Carr, M., et al. 1995, PASP, 107, 375
Reynolds, M. T., Walton, D. J., Miller, J. M., & Reis, R. C. 2014, ApJL, 792, L19
Ricci, C., Trakhtenbrot, B., Koss, M. J., et al. 2017, ApJS, 233, 17
Sheinis, A. I., Bolte, M., Epps, H. W., et al. 2002, PASP, 114, 851
Soucail, G., Fort, B., Mellier, Y., & Picat, J. P. 1987, A&As, 172, L14
Spinrad, H. 1982, PASP, 94, 397
Stern, D. 1999, PhD thesis, U.C. Berkeley
Stern, D. 2015, ApJ, 807, 129
Stern, D., Assef, R. J., Benford, D. J., et al. 2012, ApJ, 753, 30
Stern, D., Dey, A., Spinrad, H., et al. 1999, AJ, 117, 1122
Stern, D., Jimenez, R., Verde, L., Stanford, S. A., & Kamionkowski, M. 2010, ApJS, 188, 280
Stern, D., Moran, E. C., Coil, A. L., et al. 2002, ApJ, 568, 71
Tonry, J. L., & Kochanek, C. S. 2000, AJ, 119, 1078
van der Wel, A., Franx, M., van Dokkum, P. G., et al. 2005, ApJ, 631, 145
Walsh, D., Carswell, R. F., & Weymann, R. J. 1979, Natur, 279, 381
Weisskopf, M. C., Brinkman, B., Canizares, C., et al. 2002, PASP, 114, 1
Wilms, J., Allen, A., & McCray, R. 2000, ApJ, 542, 914
Winn, J. N., Lovell, J. E. J., Chen, H.-W., et al. 2002, ApJ, 564, 143
Wright, E. L., Eisenhardt, P. R. M., Mainzer, A. K., et al. 2010, AJ, 140, 1868